

## Static and Dynamic Characterization of P-N Junction Solar Cells

**A.R.M. Alamoud, H.F. Ragaie\* and B.A. Al-Mashary**

*Electrical Engineering Department, College of Engineering,  
King Saud University, P.O. Box 800, Riyadh 11421, Saudi Arabia*

*\*Ainshams University, College of Engineering, Electronics and  
Computer Department, P.O. Box 17511, Cairo, Egypt*

(Received 18 May 1996; accepted for publication 2 July 1997)

**Abstract.** This work presents an accurate, fast and automated technique for characterizing p-n junction single crystal solar cells. A PC-based system was constructed to measure the static conditions — current-voltage characteristics, and dynamic characteristics — capacitance-voltage characteristics in the reverse bias region and impedance-frequency-voltage characteristics in the forward region.

Different techniques were used to extract the model parameters as well as the most important physical and technological parameters. The five parameters single diode lumped model was used to fit the measured I-V data under AM1 illumination. The extracted parameters of the lumped model were used as an input for the PSPICE program to simulate the solar cell characteristic.

Both measurement and extraction of parameters were carried out on-line under the direct control of a personal computer. The developed system exhibits reliable performance and its use can be extended for characterizing other semiconductor devices.

### Nomenclature

- A cross-sectional area ( $\text{cm}^2$ )
- C total capacitance (F)
- $C_j$  junction (depletion-layer) capacitance (F)
- $C_s$  minority carrier storage capacitance (F)

FF	solar cell fill factor (%)
$G_{sh}$	small signal shunt conductance (V)
$I_L$	photogenerated current (A)
$I_{max}$	current at maximum power (A)
$I_s$	diode saturation current (A)
$I_{sc}$	short-circuit current (A)
n	ideality factor
$n^+$	heavily-doped n-type material
$N_A$	acceptor concentration ( $cm^{-3}$ )
Q	quality of fit factor (%)
q	electronic charge (C)
$R_s$	series resistance ( $\Omega$ )
$R_{sh}$	shunt resistance ( $\Omega$ )
$R_{sho}$	shunt resistance ( $\Omega$ ) near $V_A = 0$
$r_j$	small-signal junction shunt resistance ( $\Omega$ )
$r_s$	small-signal series resistance ( $\Omega$ )
$V_A$	applied voltage (V)
$V_{bi}$	junction built-in voltage (V)
$V_{max}$	voltage at maximum power (V)
$V_{oc}$	open circuit voltage (V)
$V_R$	reverse bias voltage (V)
$V_T$	thermal equivalent voltage (V)
$\omega$	angular frequency (rad/s)
Z	impedance ( $\Omega$ )
$\eta$	conversion efficiency (%)
$\epsilon_0$	permittivity of free space
$\epsilon_r$	relative dielectric constant of semiconductor
$\tau$	the time constant (s)
$\tau_n$	electron minority carrier lifetime (s)

## Introduction

Personal computer aided characterization (PCAC) has become a necessity in research and development because of its potential in regards to accuracy, speed, reliability and computational capabilities.

Fast and accurate determination of solar cell parameters from experimental data is very important in the design, evaluation and quality control of solar cells. Therefore the use of PCAC will be effective and powerful in that area.

PCAC used in this paper includes two main processes: (a) PC-aided data acquisition process in which both static and dynamic characteristics are measured, and (b) PC-aided data analysis process in which the measured data are used to extract the different models and physical parameters.

The static conduction characterization includes the measurement of the I-V characteristic under dark and different illumination conditions and the measurement of  $I_{sc}$ - $V_{oc}$  under very low illumination conditions. Assuming the single diode lumped model, these measured characteristics are used to extract the five model parameters ( $n$ ,  $I_s$ ,  $R_s$ ,  $R_{sh}$  and  $I_L$ ) and the output parameters (FF and  $h$ ).

The dynamic characterization includes the measurement of the C-V characteristics in the reverse bias region needed to extract the doping concentration level in the p-region and the barrier height of the device under test (DUT). Also it includes the measurement of the (Z - V - w) characteristics in the forward bias region to extract the value of the minority carriers lifetime ( $\tau_p$ ) in the p-region.

### Experimental Work

#### Measurement of the static conduction characteristics

The setup used for the measurement of the I-V characteristics is shown in Fig. 1.

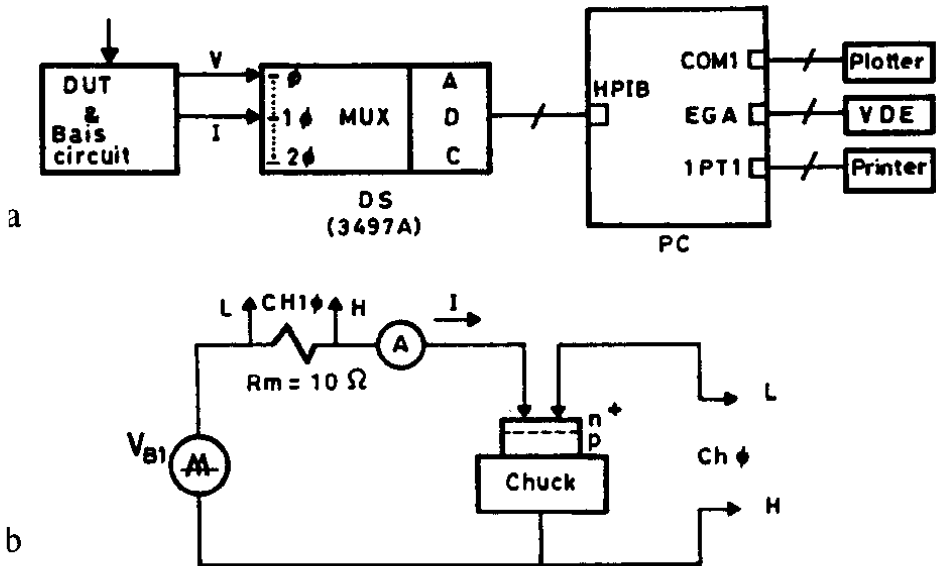


Fig. 1. (a) Block diagram for I-VA measurement setup (b) The DUT in the bias circuit using three-point probe technique.

The hardware support around the host IBM compatible PC (HP Vectra) consists of an IEEE-488 interface card (HPIB), connected to a Data Acquisition System (DAS)/Control Unit (HP 3497 A) with a built-in digital voltmeter (HP 44420 A) and a 20-Relay Multiplexer Assembly (HP 44421 A). The bias sweep voltage is obtained via a function generator (Tektronix FG-504). The maximum and minimum values of the input sweep voltage must be chosen such that it biases the cell from reverse to forward in a suitable range. The sample is connected so that the two measured quantities are fed to the DAS via two separate channels.

The contact to the cell must be implemented carefully in order to eliminate the effect of contact resistance, between the cell and the measuring probe, on the I-V characteristics. The three-point probe technique is used here, where the contact resistance effect will be decreased assuming sufficiently large back surface area.

A program was written in Basic to control the setup via the PC and to measure the I-V characteristics either under dark or under different illumination conditions.

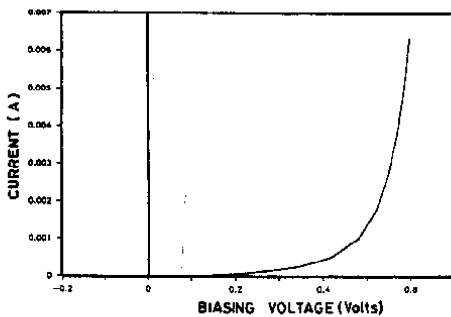


Fig. 2a. Measured I-V<sub>A</sub> characteristics of the solar cell in dark

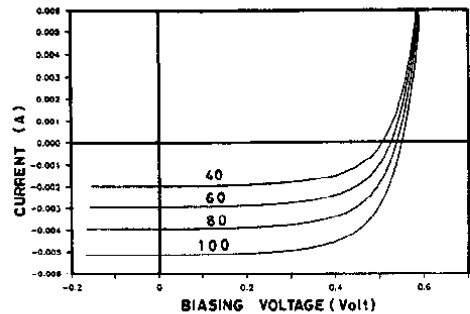


Fig. 2b. Measured I-V<sub>A</sub> characteristics of the solar cell under illuminations

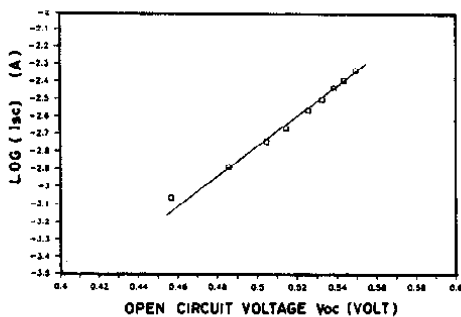


Fig. 2c. Log( $I_{sc}$ ) vs.  $V_{oc}$  at different illuminations

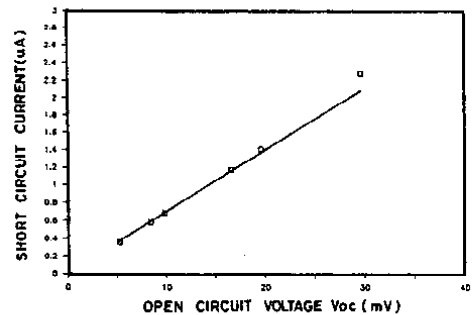


Fig. 2d. Log( $I_{sc}$ ) vs.  $V_{oc}$  at very low illumination conditions

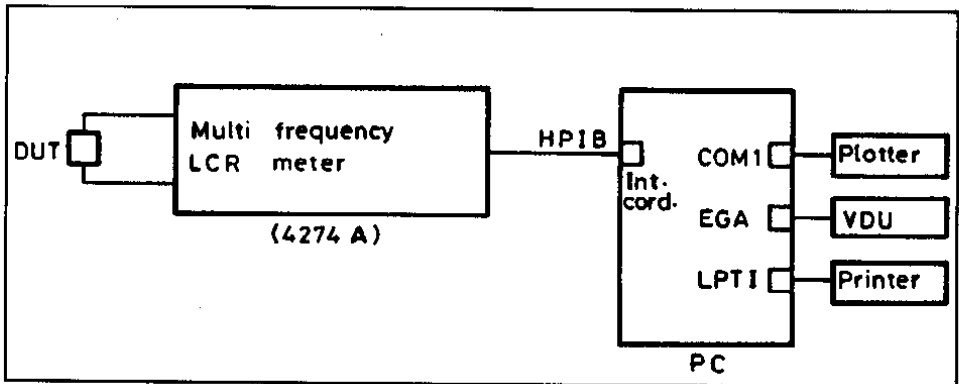


Fig. 3. Block diagram of the  $C-V_A$  measurement setup.

A  $0.18 \text{ cm}^2$  single crystal  $n^+p$  solar cell specimen has been characterized, using the setup of Fig. 1 and the Basic program. Typical results are shown in Fig. 2.

#### Measurement of the capacitance-voltage characteristic

The C-V measuring setup is shown in Fig. 3. The multi-frequency LCR meter (HP 4274A) can be programmed via the PC using the HP1B interface bus to measure the C-V characteristics of the sample in the reverse bias region at different frequencies. It can provide the small signal as well as the dc bias internally. Figure 4 shows measured C-V characteristics using the setup of Fig. 3. It is important to mention here, that the measured capacitance almost represents the depletion capacitance because the diffusion capacitance under reverse biasing is very small and the frequency of measurement is low.

#### Measurement of the impedance-voltage-frequency characteristics

The measurement set up is shown in Fig. 5. The lock-in amplifier (LIA) (ITHACO 362 A) is used because of its ability to measure very small signals (amplitude and phase) with respect to a reference signal. It is controlled through the PC using the HP1B interface bus. The LCR meter is used to provide both the programmed small signal and the forward dc bias voltage to the sample. The small signal is also used as a reference signal for the LIA.

Through the LIA, the PC can measure two signals that are proportional to the voltage across the sample and the current through it. By this measurement the forward impedance is calculated easily using Ohm's law. Typical results are given in Fig. (6).

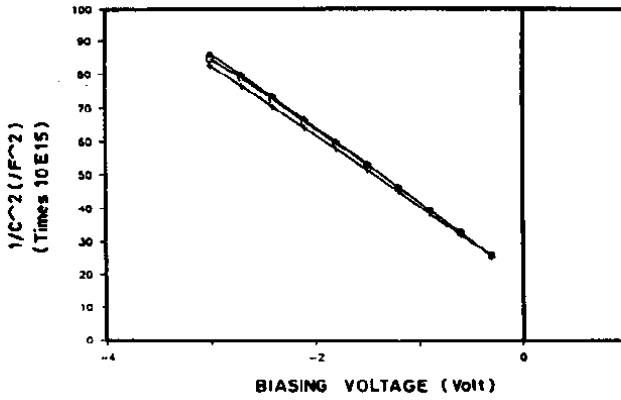


Fig. 4a. The measured  $(1/C^2)$ -V at different frequencies

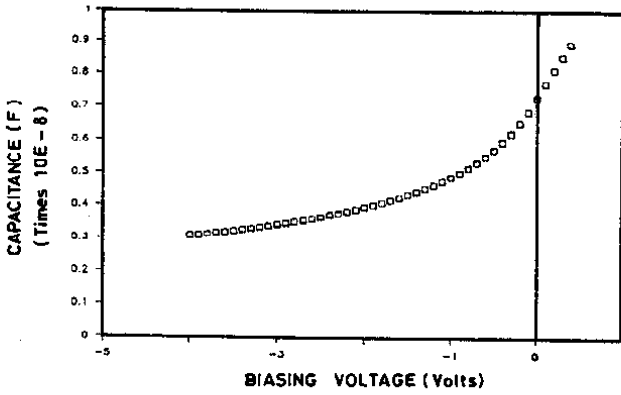


Fig. 4b. C-V characteristics

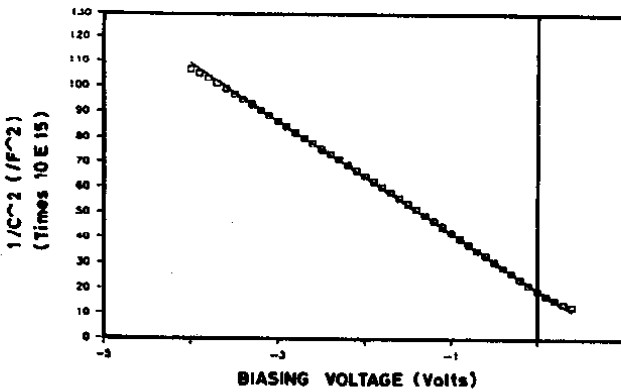


Fig. 4c.  $(1/C^2)$  vs V characteristics.

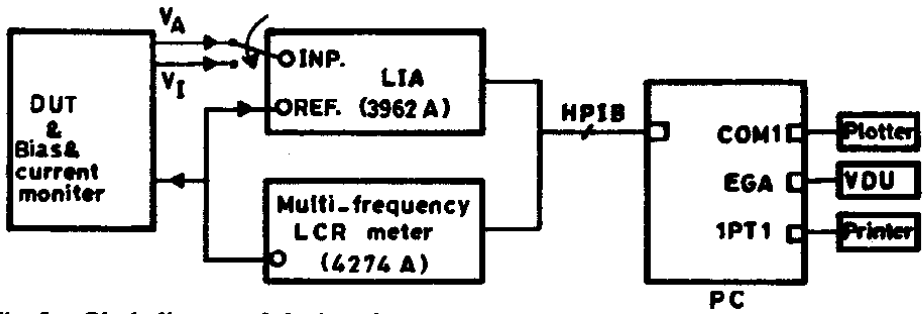


Fig. 5a. Block diagram of the impedance measurement setup.

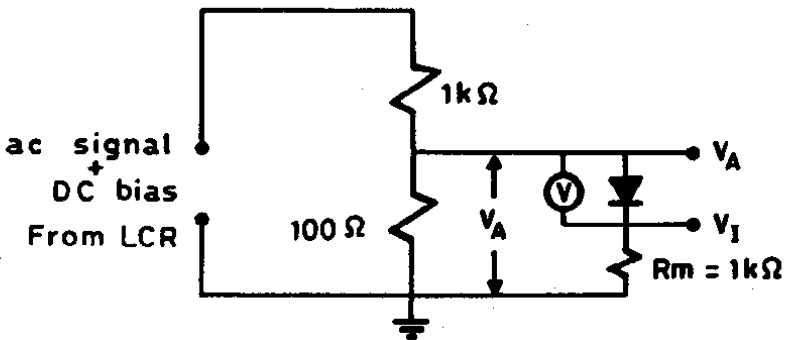


Fig. 5b. Connection of the DUT and the bias circuit.

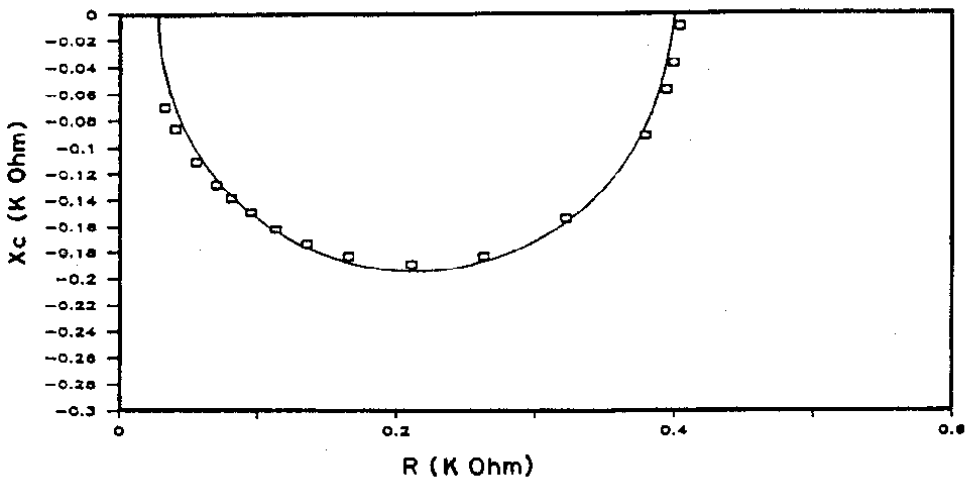


Fig. 6. Impedance diagram at  $V_A = 0.35$  V.

## Parameter Extraction and Discussion

### I-V Characteristic under dark condition

The measured I-V characteristics shown in Fig. 2a can be used to extract the parameters of the single diode model of the solar cell shown in Fig. 7 [1,2]. The general relation between the current and voltage of the solar cell can be written in the following form [1]

$$I = I_s [e^{(V_A - IR_s)/nV_T} - 1] + \frac{(V_A - IR_s)}{R_{sh}} \quad (1)$$

$$\text{where } V_T = \frac{kT}{q} = \frac{T}{11600}$$

In most solar cells  $R_s/R_{sh} \ll 1$ , so Eq. 1 takes the form

$$I = I_s [e^{(V_A - IR_s)/nV_T} - 1] + \frac{V_A}{R_{sh}} \quad (2)$$

Equation (2) can be used at different regions of current values to extract certain parameters in the regions where these parameters are dominant.

The experimental I-V characteristic of Fig. 2a can be approximated near the origin by a straight line to extract  $R_{sh}$ . The Log (I)-V plot shown in Fig. 8 can be approximated by a straight line in the medium current region to extract  $I_s$  and  $n$ .  $R_{sh}$  and  $R_s$  can then be found at each bias voltage in both low and high current regions respectively.

It was found that  $R_s$  and  $R_{sh}$  values vary with bias as shown in Fig. 9, so their average values are calculated. Table 1 summarizes the results of the analysis described above.

The extracted parameters of the lumped model are used as an input for the PSPICE program to simulate the solar cell characteristics. Figure 10 shows good matching between the simulated and measured characteristics. The increase in the  $R_s$  lumped value could be explained by the distributed nature of the cell equivalent circuit. The bias voltage distribution is not uniform over the cell surface (current crowding effect) [3]. On the other hand, the decrease of  $R_{sh}$  with bias has also been reported in the literature [4]. It might be caused by metal spikes penetrating the top layer causing Schottky-like barriers.

### The I-V Characteristics Under Illumination Conditions

Two methods for extracting the solar cell parameters under illumination are presented in this section [5].



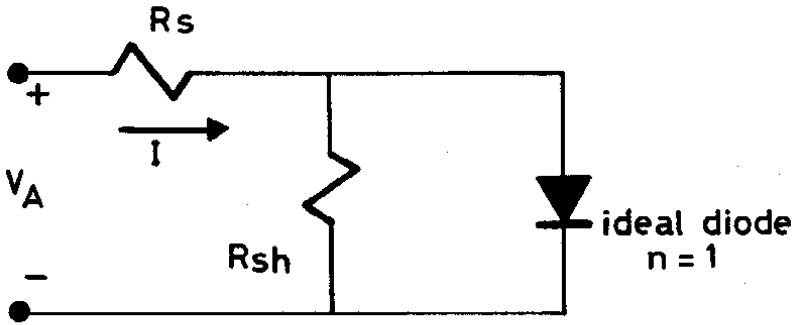


Fig. 7. Static condition model.

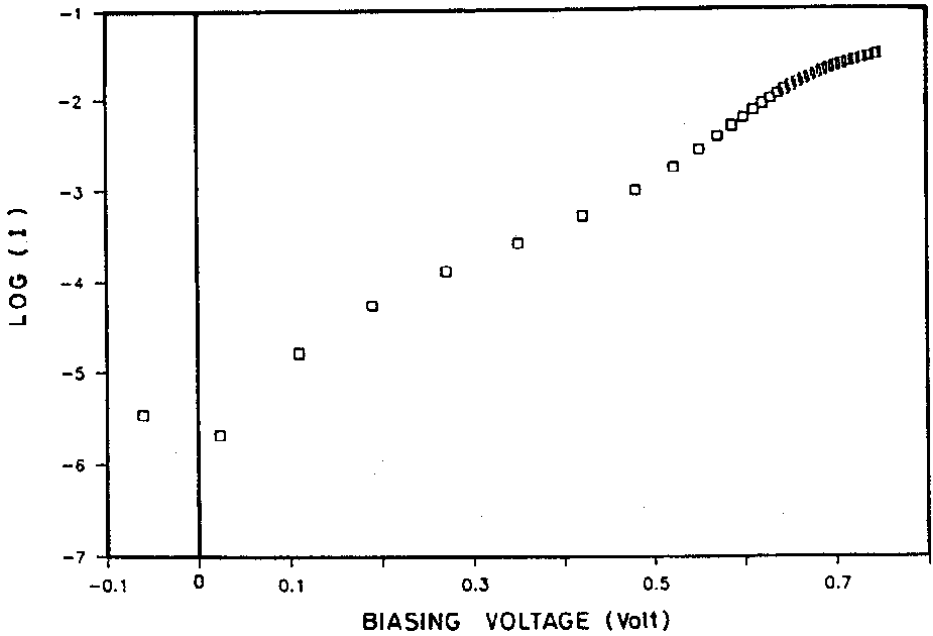


Fig. 8. Log (I) vs bias voltage at dark condition.

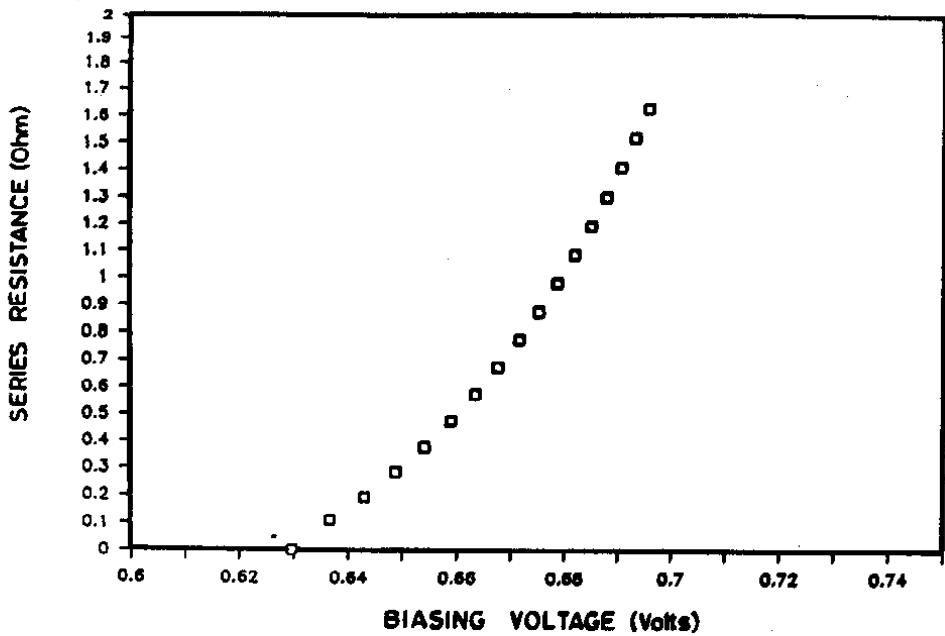


Fig. 9a. Equivalent lumped series resistance vs bias voltage.

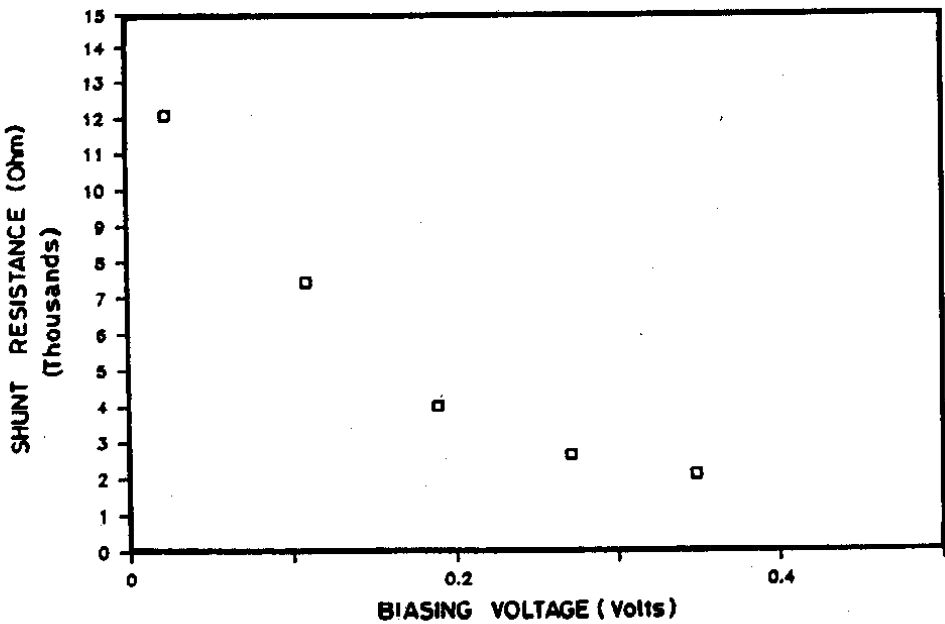


Fig. 9b. Equivalent lumped shunt resistance vs bias voltage.

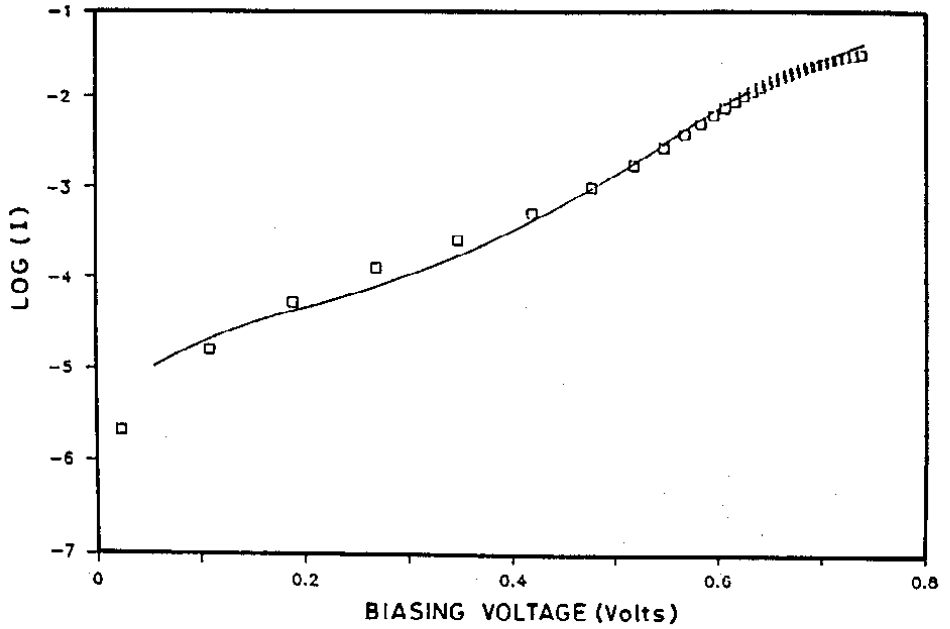


Fig. 10. PSPICE simulation of the extracted lumped model

A) Analytical method

The mathematical relation between the  $I_{sc}$  and  $V_{oc}$  under high illumination conditions can be shown to have the following form,

$$I_{sc} \cong I_s e^{V_{oc}/nV_T} \tag{3}$$

Table 1. Single-diode model extracted parameters under dark condition

$I_s$	$n$	$R_{sho}$	$R_{sh} (av.)$	$R_s (av.)$
(A)		(kW)	(W)	(kW)
$3.12E-7 \pm 4.2E-9$	$2.333 \pm 0.017$	$13.34 \pm 2.5$	1.3	5.65

Table 2. Single-diode model extracted parameters under illumination using analytical method

$I_s$	$n$	$R_{sho} (av.)$
(A)		(kW)
$2.03E-7 \pm 1.15E-8$	$2.12 \pm 0.08$	$13.77 \pm 0.0$

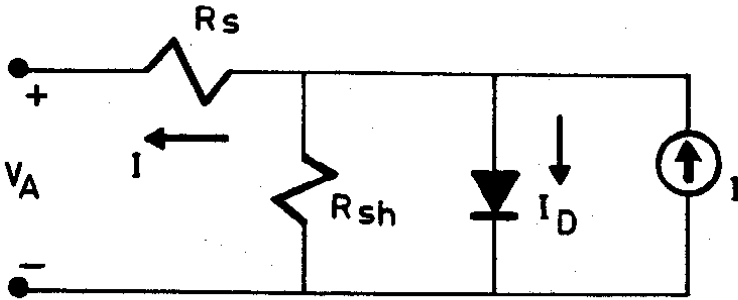


Fig. 11. Solar cell five parameters single diode lumped model.

Thus if the  $\log(I_{sc}) - V_{oc}$  characteristic shown in Fig. 2c is approximated by a straight line,  $I_s$  and  $n$  can then be extracted directly. But the mathematical relation between  $I_{sc}$  and  $V_{oc}$  under very low illumination conditions can be written in the following form,

$$I_{sc} \cong \frac{V_{oc}}{R_{sho}} \quad (4)$$

which means that if the  $I_{sc} - V_{oc}$  characteristics shown in Fig. 2d is approximated by a straight line,  $R_{sho}$  can be easily extracted. The analysis results are summarized in Table 2.

### B) Curve fitting techniques

Another approach is followed here to extract all the parameters of the solar cell model from the whole set of measured I-V characteristics using fitting techniques. The five parameters single diode lumped model shown in Fig. 11 is used to fit the measured I-V data under AM1 illumination ( $100 \text{ mW/cm}^2$ ).

The numerical algorithm used in the proposed fitting technique is given in literature [1]. The fill factor and efficiency can also be calculated. Table 3 represents the output list of the fitting program while Fig. 12 shows the experimental points over the generated fitting curve.

## C-V Characteristics

It is clear from Fig. 4a, that the measured capacitance under reverse bias voltage is independent of the small signal frequency and represents the junction (depletion-layer) capacitance directly.

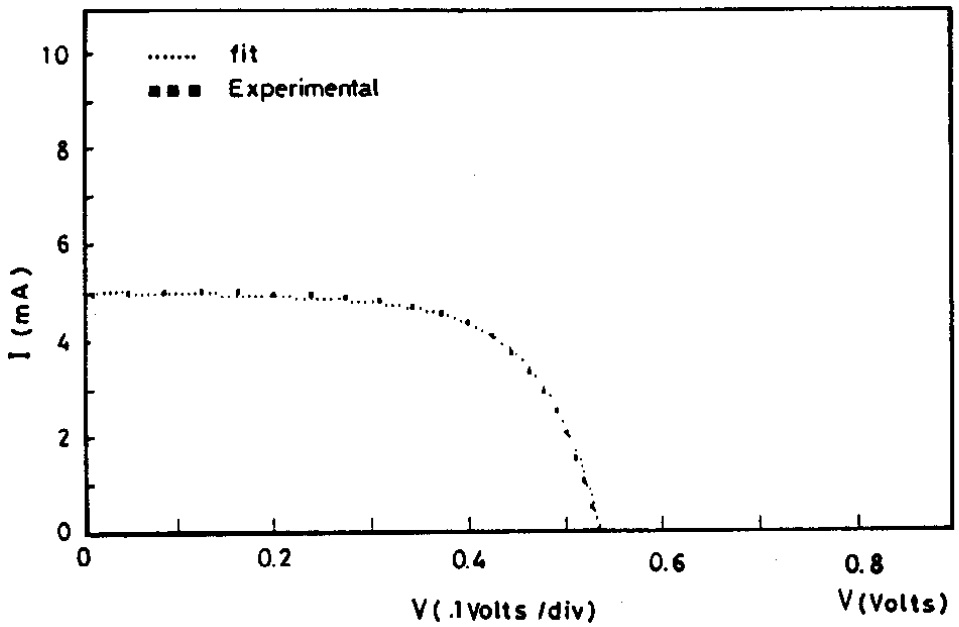


Fig. 12. Plot of the best fit over the measured data points.

Table 3. Solar cell extracted parameters using fitting techniques

$I_L$ (A)	5.00E-03
$I_S$ (A)	5.20E-07
B	16.97
n	2.27
$R_S$ ( $\Omega$ )	0.21
$G_{sh}$ ( $\mu$ )	0.00063
N	65
$N_I$	55
Fit factor (%)	88.13
$I_{SC}$ (A)	4.97E-03
$V_{OC}$ (V)	0.536
$I_{max}$ (A)	4.16E-03
$V_{max}$ (A)	0.411
FF (%)	64.1
$\eta$ (%)	14.9 (active area)

The general relation between the capacitance and the bias voltage for any p-n junction is,

$$\frac{1}{C_j^2} = -\frac{2}{q\epsilon_r\epsilon_0 A^2 N_A} (V_R - V_{bi}) \quad (5)$$

or

$$\frac{1}{C_j} = \frac{1}{BN_A} (V_R - V_{bi}) \quad (6)$$

where

$$B = \frac{q\epsilon_r\epsilon_0 A^2}{2}$$

If the measured points of Fig. 4c are approximated by a straight line to represent the relation (6), the doping concentration in the base ( $N_A$ ) and the barrier height ( $V_{bi}$ ) can be extracted. The following values are obtained respectively,

$$\begin{aligned} N_A &= 1.68E16 \pm 4.3E12 \text{ cm}^{-3} \\ V_{bi} &= 0.88 \pm 0.02 \text{ V} \end{aligned}$$

We should point out here that the error  $\pm 4.3E12 \text{ cm}^{-3}$  in  $N_A$  is due to the fitting of the experimental data with a straight line. Other sources of errors, such as estimating the cell area are not considered.

The relatively high value of the barrier height voltage ( $V_{bi}$ ) is due to the highly doped top layer of the ( $n^+$ -p) junction under test.

### Z-V- $\omega$ Characteristics

The small signal model of the p-n junction solar cell at forward bias is shown in Fig. 13. The total impedance expression can be written at certain forward bias as follows:

$$Z = [r_s + \frac{r_j}{1 + \omega^2 c^2 r_j^2}] - j [\frac{r_j^2 c \omega^2}{1 + \omega^2 c^2 r_j^2}] \quad (7)$$

$$Z = R(\omega) - jX_c(\omega) \quad (8)$$

where  $C = C_j + C_s$  and  $r_j = 1/G$

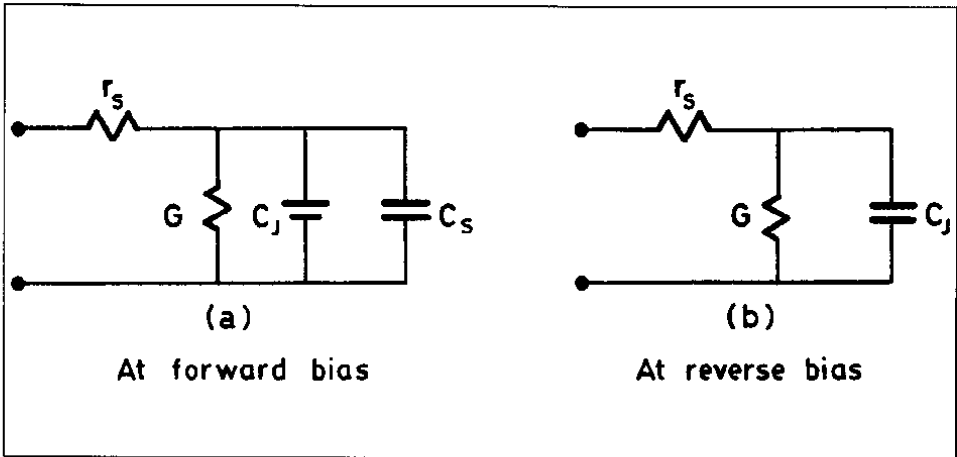


Fig. 13. Small signal model of a p-n junction

We should mention here that minority carriers storage capacitance includes the effect of the minority carriers in the neutral region (usually called diffusion capacitance) and the minority carriers in the depletion region (usually called space charge recombination capacitance). The expressions of these capacitances are given in [6] and [7].

The impedance locus in the  $R-X_c$  plan represents a semicircle as shown in Fig. 6. In this figure, the following relations apply

$$\tan f = r_j C_w \tag{9}$$

at  $f = 45^\circ \quad r_j C_w = 1 \tag{10}$

then  $t = r_j C = 1/w \quad \text{at } f = 45^\circ \tag{11}$

The minority carriers lifetime is given by

$$t_n = r_j C_s \tag{12}$$

so  $t_n = t - r_j C_j \tag{13}$

Using the impedance diagram in Fig. 6, the value of  $t$  can be calculated using equation (11) and the value of  $r_j$  can be estimated graphically. The value of the junction capacitance ( $C_j$ ) at this bias can be found by extrapolating the straight line in Fig. 4c to the forward bias region. Equation (13) can then be used to calculate the value of the lifetime ( $t_n$ ). Table 4 lists the calculated small signal parameters at a forward bias of 0.35V.

**Table 4. Calculated small signal parameters at 0.35 V forward bias**

$r_s$ ( $\Omega$ )	$r_s + r_j$ ( $\Omega$ )	$r_j$ ( $\Omega$ )	$\omega$ at $\phi=45$ (kHz)	$\tau$ ( $\mu\text{sec}$ )	$C_j$ (F)	$\tau_n$ ( $\mu\text{sec}$ )
30	400	370	38.2	4.166	0.91 E-8	0.799

Since the ideality factor obtained from the I-V characteristics is approximately 2, the recombination current component is the dominant one. Therefore we can speak about space charge capacitance rather than the diffusion capacitance. Also, the life time ( $\tau_n$ ) obtained from this measurement will represent mainly the life time of minority carriers in the space charge region.

The calculation of  $C_s$  has been made at relatively low frequency (less than 50 kHz), which satisfy the low frequency condition ( $\omega \tau \ll 1$ ). Therefore  $C_s$  is considered independent of frequency.

### Conclusions

A PC-based data acquisition system for characterizing a two-terminal solid state device is implemented. The system can be used to measure the current-voltage characteristics under both dark and illumination conditions, the capacitance-voltage characteristics and the impedance-frequency characteristics of p-n junction diode. The system has been used to measure with high speed and reliability the different characteristics for single crystal as well as polycrystalline silicon solar cells.

The measured data have been used to characterize the samples either by analysis or fitting techniques using a PC in order to extract the different solar cell parameters. The fitting program which was designed to extract the cell parameters from the illuminated I-V characteristics can be considered an accurate and fast approach for the characterization of the p-n junction solar cells.

It was found that recombination current component is dominant over diffusion component of current. Moreover, the device capacitances showed frequency independence up to 100 kHz.

### References

- [1] Nguyen P.H., Lepley, B., Boutrit, C. and Ravelet, S. "Computer Aided-Characterization of the Illuminated and Dark Current-Voltage Characteristics of Solar Cells". *2nd European Community Photovoltaic Conference*, 1979, 492-502.
- [2] Golio, M. "Characterization, Parameter Extraction and Modeling for High Frequency Applications". *23rd European Microwave Conference Proceedings*, Vol. 1 (1993), 69-72, 1993.
- [3] Fahrenbruch, A.L. and Bube, R.H. *Fundamentals of Solar Cells*. Academic Press, 1983.
- [4] Chan, D.S.H. and Phang, J.C.H. "A Method for the Direct Measurement of Solar Cell Shunt Resistance".



- IEEE Transaction on Electron Devices*, Vol. ED-31, (1984), 381-383.
- [5] Ragaie, H.F. and Alamoud, A.R.M. "PC-Aided Characterization of Solar Cells". *2nd ASRE*, March 19-22, 1989, Cairo, Egypt.
- [6] Arnost, N., Pao-Jung, C., Shing-Chong, P. and Fredrik, A.L. "Diffusion Length and Lifetime Determination in p-n Junction Solar Cells and Diodes by Forward-Biased Capacitance Measurements". *IEEE Transactions on Electron Devices*, Vol. ED-25, No. 4 (1978), 485-490.
- [7] Zekry, A.H. and Al-Mazroo, A.Y. "A Distributed SPICE-Model of a Solar Cell". *IEEE Transactions on Electron Devices*, Vol. 43, No. 5 (1996), 691-700.

## تمييز الخصائص المستقرة والحركية لخلايا شمسية ذات وصلة من نوع P - N

عبدالرحمن العمود، هاني فكري رجائي\* و بندر عبدالله المشاري  
قسم الهندسة الكهربائية، كلية الهندسة، جامعة الملك سعود، ص. ب ٨٠٠،  
الرياض ١١٤٢١، المملكة العربية السعودية  
و \* قسم الألكترونيات و الحاسبات، كلية الهندسة، جامعة عين شمس،  
ص.ب ١٧٥١١، القاهرة، جمهورية مصر العربية  
(أستلم في ١٨/٥/١٩٩٦م؛ وقبل للنشر في ٧/٧/١٩٩٧م)

**ملخص البحث.** يقدم هذا البحث أسلوبًا تقنيًا يتميز بالسرعة والدقة والتلقائية لتمييز الخصائص الكهربائية لخلايا شمسية ثنائية الوصلة. تم بناء نظام يعتمد على الحاسب الشخصي لقياس خصائص الحالة المستقرة (التيار - الفولتية)، والخصائص الحركية: السعة - الفولتية، في حال الانحياز العكسي، وخصائص المعاوقة الذبذبة - الفولتية، في حال الانحياز الأمامي.

استخدمت أساليب مختلفة لاستخلاص متغيرات النموذج بالإضافة إلى أهم المتغيرات الفيزيائية والتقنية. وتم استخدام نموذج مجمع للثنائي المفرد لاستخلاص الخصائص من بيانات التيار - الفولتية، المقاسة تحت إضاءة AM1. تلا ذلك استخدام هذه المتغيرات كمدخلات لبرنامج PSPICE لتمثيل خصائص الخلية الشمسية.

أجريت جميع القياسات واستخلصت جميع المتغيرات مباشرةً بواسطة الحاسب الشخصي. وقد أظهر النظام المطور أداءً موثوقًا يمكن توسيع استخدامه لتمييز خصائص نائط أشباه موصلات أخرى.